ANNALS OF GEOPHYSICS, 68, 5, DM579, 2025; doi:10.4401/ag-9279
OPEN ACCESS

DIVEnet: a local seismographic network monitoring the lower continental crust drilling activities for the ICDP-DIVE project

Judith M. Confal[1], Simone Salimbeni[1], Adriano Cavaliere[1], Stefania Danesi[1], Irene Molinari[1], Maddalena Errico[1], Ludovic Baron[2], Steffen Uhlmann[3], György Hetényi[2], Silvia Pondrelli[*,1]

(1) Istituto Nazionale di Geofisica e Vulcanologia, Bologna, Italy
(2) University of Lausanne, Institute of Earth Sciences, 1015 Lausanne, Switzerland
(3) IGM GmbH, Untere Sankt Leonhard Strasse 16, Uberlingen, Germany

Article history: received January 29, 2025; accepted July 3, 2025

Abstract

The ICDP DIVE project (Drilling the Ivrea-Verbano zonE) addresses fundamental questions about the nature of the lower continental crust and its transition to the mantle. In its first phase, the project has drilled two, scientific, fully cored boreholes in the Ivrea Verbano Zone (IVZ) in Italy. The IVZ, considered the world's best outcrop of lower crustal continental rocks, is structurally and historically connected to the underlying Ivrea Geophysical Body, a major, high density and high seismic-velocity anomaly studied since the 1960s and a characteristic feature of the Western Alps. The two boreholes were conducted between 2022-2024 in Val D'Ossola: the first in Ornavasso and the second in Megolo, 7 km apart. Within this framework, a dedicated seismographic network, named DIVEnet, has been monitoring natural earthquakes and possible operation-related seismic activity for three years. Eleven seismographic stations (short period and broadband), provided by INGV and the University of Lausanne, were installed within a maximum distance of 15 km from the midpoint between the two drilling sites. All stations recorded data continuously and 10 provided data in real time. One broadband sensor was installed in a borehole, and its horizontal components' orientation was determined by multiple methods. The stations occupied 14 different locations and operated from autumn 2021 to summer 2024, with varying recording durations. Being in an area characterized by low natural local seismicity and a relatively sparse distribution of seismographic stations, it is particularly important to record background activity and noise for as long as possible, especially before and after the start of drilling activities. Daily monitoring was conducted at INGV in quasi real time, and probabilistic power spectral density distributions (PPSD) have been computed. In total, 28 events with magnitudes ranging from 0 to 2.6 MLv were recorded within a distance of about 20 km from the boreholes, most of them aligned with the Insubric Line, that is thought to be tectonically inactive, and 612 events were recorded in the larger study region. No events were related to the drilling activities, which have only very slightly increased noise levels, mostly in the 0.1-0.3 Hz frequency range.

Keywords: Temporary networks, Seismic monitoring, Borehole sensors direction, Anthropic activities

1. Introduction

The Ivrea-Verbano Zone (IVZ) in the Italian Alps is one of the most complete and best-studied examples of an exposed continental crust-upper mantle transition on Earth (Spicher, 1968; Salisbury and Fountain, 1990; Pistone et al., 2020, and references therein). To the west-northwest, the IVZ is bounded by the South Austroalpine domain along the Oligocene-Miocene Insubric Line (Schmid et al., 1987; Nicolas et al., 1990; Berger et al., 2012). To the east, it is juxtaposed against middle to upper crustal rocks by two major faults: the Cossato-Mergozzo-Brissago (Permian, Snoke et al., 1999) and the Pogallo (Late Permian to Early Jurassic; Handy, 1987; Boriani et al., 1990; Garde et al., 2015) (Fig. 1). The increase in the metamorphic grade towards the northwest, the steep foliations that are sub-parallel to the Insubric Line (Quick et al., 1992), and the available thermobarometric estimates (Redler et al., 2012) demonstrate that the IVZ represents a tilted, preserved cross-section of lower continental crust.

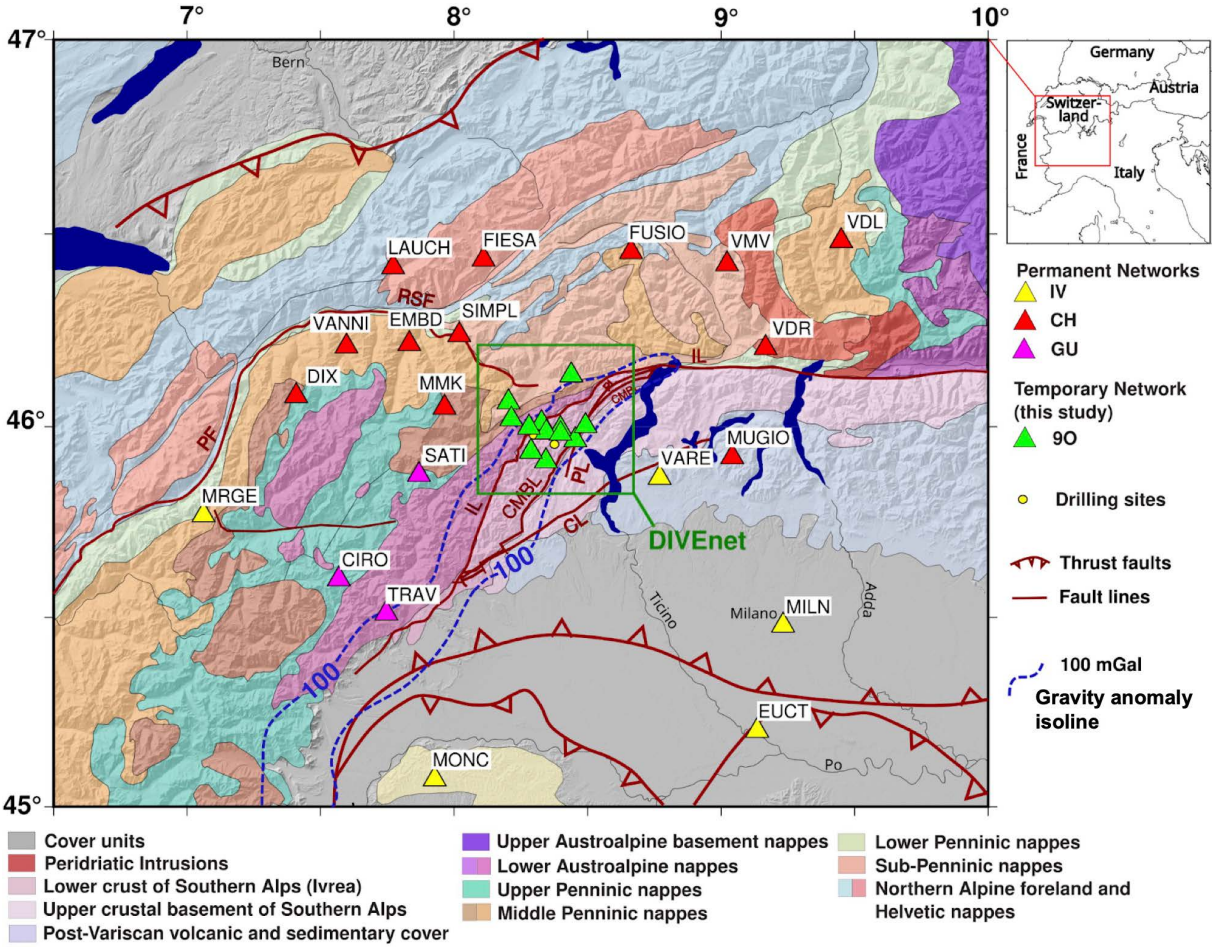

Figure 1. Temporary (light green triangles) and permanent stations (yellow, red and pink triangles) used for monitoring. The names of permanent stations are plotted beside the symbols. The temporary DIVEnet and drillings sites (yellow dots) are shown in detail in Fig. 2. Geological features are after Schmid et al. (2004; 2017) showing roughly the geological units in transparent colours over the topography. The underground Ivrea Geophysical Body (IGB) is represented by the 100 mGal gravity anomaly isolines of Scarponi et al. (2020). Main tectonic features are drawn with red lines after Schmid et al. (2017) and Petri et al. (2019). CL: Canavese Line, CMBL: Cossato-Mergozzo-Brizzago Line, IL: Insubric Line, RSF: Rhône-Simplon Fault, PF: Penninic Front, PL: Pogallo Line.

The Ivrea Geophysical Body (IGB) is a segment of Adria's upper mantle located at shallow depth, responsible for the largest positive gravity anomaly in the Alps (Schmid et al., 1987, 2004; Kissling, 1984; Masson et al., 1999; Paul et al., 2001; Béthoux et al., 2007; Scarponi et al. 2020, 2021, 2024). The projection at the surface of the underground structure of the IGB, following the isolines of the Ivrea gravity anomaly, extends roughly from Locarno

in southern Switzerland to the vicinity of the Ligurian Sea, following the arcuate shape of the mountain belt near the topographic transition. The 3D reconstruction obtained with a joint inversion of gravity and seismic data (Scarponi et al., 2021) shows that the IGB model dips steeply near the surface, typically towards the Adria plate, and flattens to sub-horizontal at a depth of approximately 30 km beneath the Po Plain. The IGB geometry is confirmed by the presence of distinct magnetization, high density, and high seismic velocity associated with the upward intruding shape of the anomaly at or near the surface, locally at ~1±1 km depth b.s.l. (Scarponi et al., 2020, 2021). These observations suggest that the IVZ and the IGB were tectonically deformed and brought respectively to surface and to shallow depth as a result of the Adria-Europe collision. With mantle material at and just below the surface, the IVZ provides an excellent opportunity to connect geophysical and geological scales by utilizing physical, chemical, and mineralogical data collected from drill cores, downhole logging, and local or regional field surveys. The primary goal is to develop integrated petrological and geophysical models to better understand the nature and evolution of the continental lower crust and the Moho transition zone. Two boreholes were drilled as part of the phase 1 of ICDP-DIVE project (www.dive2ivrea.org, https://www.icdp-online.org/projects/by-continent/europe/dive-italy), near Ornavasso and in Megolo di Mezzo (Greenwood et al. 2024), reaching depths of 578.5 m (5071_1_B, October-December 2022, marked with 1B in Figures) and 909.5 m (5071_1_A, October 2023-April 2024, marked with 1A in Figures), respectively, under ICDP expedition number 5071. Given that the deep boreholes were realized in an active Alpine region near the Insubric Fault, a temporary seismographic network, named DIVEnet (FDSN network code: 9O) was installed to monitor any anomalous seismicity potentially related to the drilling activities. The network also aimed to improve the understanding of seismic activity in the region, which is characterised by earthquakes occurring along fault systems in Switzerland and Italy (e.g. the Rhône-Simplon fault and the Canavese line, Bagagli et al., 2022). In contrast to regions in close proximity to the drill sites and the Val D'Ossola, the seismicity is generally considered to be low, both historically and in the present day (e.g., Bagagli et al., 2022; Rovida et al., 2022), with no particular pattern associated with mapped faults observed.

In the following sections, the setup and operation of this temporary network are described, the quality control processes are explained, and the results from three years of seismic data collection in the region and real time location and monitoring are presented.

2. Description of the Network

DIVEnet is a temporary seismological network established to monitor the region during drilling operations at two scientific boreholes, which were deepened using diamond-coated drill bits and recovered 100% of cores. Eleven seismic stations were installed around the proposed drilling sites, with nine becoming operational in October 2021 and two additional stations starting in January 2022 (Table 1). Some stations were relocated during the project to optimize the network geometry for the second borehole phase at 5071_1_A near Megolo (e.g., DIV05 and DIV10). Most stations were dismantled in June 2024, with two continuing to record until August 2024, while DIV07 remains still operational. Data acquisition has been managed by INGV Bologna, with additional support from INGV Pisa for the acquisition process.

The network was designed with the midpoint between the two drilling sites as the system's barycenter, maintaining an interstation distance between 10 to 15 km. The installation locations were identified with the assistance of local authorities and administrations, who provided public spaces such as unused schools, churches, or cemeteries in small villages (see Fig. 2 for photographs). All sites were accessible by car year-round, had access to mains power to avoid reliance on solar panels, and supported cellular data (GSM) signals for real-time data transmission (except DIV12). This setup minimized the need for frequent site visits and ensured consistent monitoring, though some sites were subject to higher noise levels. Despite these challenges, remote locations were identified that produced reliable results and facilitated efficient maintenance operations.

As shown in Fig. 2, DIVEnet had a predominantly east-west axis of deployment. This configuration was determined by the positions of the drill sites, the morphology of the Ossola Valley, and the proximity of remote and protected Valgrande National Park (between DIV02 and DIV11), where the access was either limited or impossible, and necessary infrastructure such as power and cellular data signal was unavailable. DIV12, the easternmost station, was located at the entrance to Valgrande National Park and had power, but lacked real-time data transmission capabilities. DIV11, the northernmost station, was installed in the Vigezzo Valley and provided an important complement to the east-west axis. The network included a variety of instruments (Table 1). High corner-frequency

Table 1. Station locations, recording times, site coordinates, site of installation and sensor types of the DIVEnet (Fig. 2). Trilliums are Nanometrics sensors.

Station Name	Location	Start date	End date	Lat. (°N)	Lon. (°E)	Elev. (m)	Installation place	Sensor
DIV01	Anzola	11/10/2021	07/06/2024	45.98671	8.345198	700.0	Church	SARA SS02
DIV02	Colloro	13/10/2021	03/09/2024	46.010724	8.327315	588.0	Basement	Trillium Horizon
DIV03	Nibbio	11/10/2021	12/05/2022	45.966128	8.453883	190.0	Cemetery	SARA SS02
DIV03	Nibbio	12/05/2022	26/07/2023	45.995258	8.398007	229.9	Cemetery	SARA SS20
DIV04	Bracchio	11/10/2021	04/06/2024	45.966128	8.453883	321.0	Cemetery	SARA SS02
DIV05	Ornavasso	15/09/2023	03/09/2024	45.983238	8.398803	222.0	Borehole	Trillium 120 Slim Posthole with Holelock
DIV06	Forno	11/10/2021	20/06/2024	45.93588	8.28779	906.0	Basement	SARA SS20
DIV07	Luzzogno	19/10/2021	11/05/2022	45.911285	8.3441	690.0	Cemetery	SARA SS20
DIV07	Luzzogno	11/05/2022	—	45.911301	8.344162	741.0	Cemetery	Trillium Horizon
DIV08	Seppiana	26/01/2022	05/06/2024	46.0649	8.2037	616.0	Basement	Lennartz 3D
DIV09	Castiglione	15/10/2021	06/06/2024	46.020493	8.214117	515.0	Basement	SARA SS20
DIV10	Loro	27/07/2023	06/06/2024	45.998585	8.280583	240.0	Church	SARA SS20
DIV11	Druogno	17/11/2021	03/09/2024	46.135147	8.438736	894.0	Cemetery	Trillium Compact
DIV12	Cicogna	25/01/2022	19/06/2024	46.0032	8.492	775.0	House	Lennartz 3D

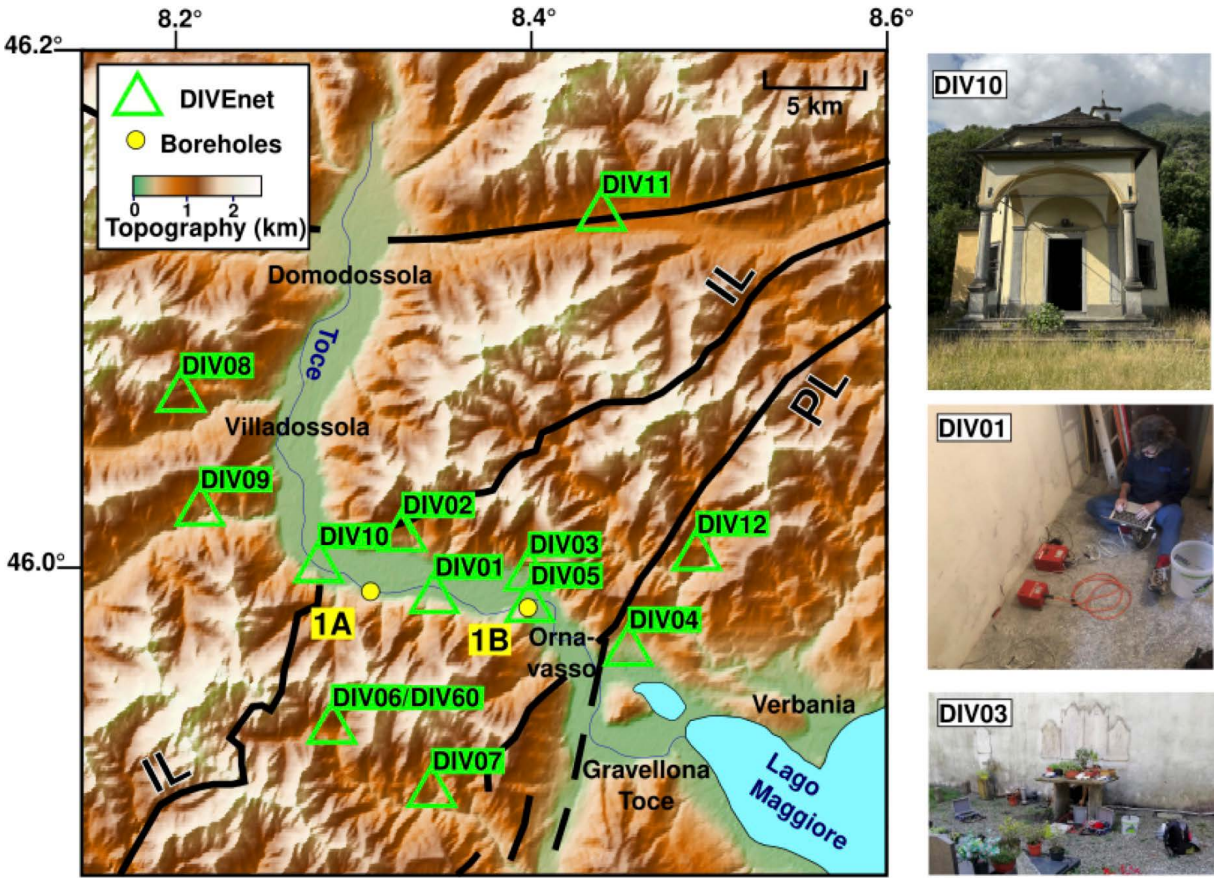

Figure 2. Map of DIVEnet stations (green triangles) and the drilling sites (yellow dots). Drill site 1B corresponds to 5071_1_B, which operated between October to December 2022 and 1A corresponds to drill site 5071_1_A, active between October 2023 to April 2024. See Table 1 for station locations. Fault lines are after Brack et al. (2010). IL: Insubric Line, PL: Pogallo Line.

sensors (e.g., SARA sensors with characteristic periods of 0.5 and 5 seconds) were installed closer to the drill sites, such as at DIV01 (Fig. 2). From late 2023, the Trillium 120 Slim Posthole sensor, initially deployed at Forno under the station name DIV60 and co-located with DIV06, was moved to the 5071_1_B drill hole near Ornavasso, at a depth of 252 m below the surface. Once relocated and installed in the borehole (clamped), the station was renamed DIV05. The orientation of its horizontal components was redefined as part of the installation and dismantling process, which is described in detail in a later section.

3. Data Quality

Throughout the operation of the DIVEnet network, we periodically computed the data completeness (Fig. 3) and probabilistic power spectral density (PPSD, Figs. 4 and S1 in the supplementary material) of background seismic noise recorded on the EHZ/HHZ channels for the 13 sites and 14 stations (Fig. 2). Overall, data quality control yielded mostly good results, especially considering the temporary, straightforward, and cost-effective nature of the installations. In a few cases the PPSD shows noise anomalies at specific frequencies, that mainly were related with seasonal changes in stream water fluxes or similar natural causes. The only site with significant noise issues was DIV03, located in the village of Nibbio, northeast of the 5071_1_B drilling site near Ornavasso. Unfortunately, intermittent rock extraction activities near the cemetery – activities that were inactive during the pre-installation survey – compromised the quality of the recorded signal (Fig. S1). Additionally changing the sensor from a SARA 5s to a 0.5s has been tried, as well as burying the sensor, but the situation did not improve. Consequently, we moved the instrument from DIV03 to DIV10 after the first phase of drilling. This adjustment improved network coverage during the 5071_1_A drilling operations and resulted in better data quality.

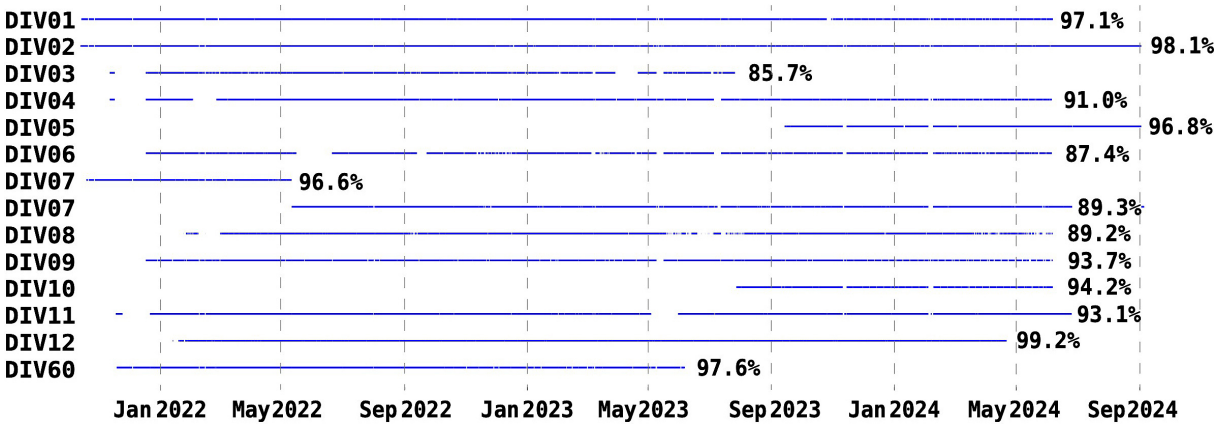

Figure 3. Data completeness for vertical channels of DIVEnet stations.

In a network with a wide variety of sensors, each with different frequency sensitivities, PPSD plots are essential for understanding the limitations and capabilities of each station. Short-period sensors (Fig. S1) exhibit low noise levels at high frequencies but show increased noise at lower frequencies (period beyond 5-10 s). In contrast, broadband and posthole sensors (Fig. 4) demonstrate acceptable noise levels over their full nominal frequency bandwidth.

There does not appear to be any significant effect on the recorded noise levels due to drilling activities (Fig. 5). During drilling at the first borehole (October 8, 2022, to December 20, 2022; Julian days 281-354), the PPSDs indicate only minor differences at the four stations closest to the Ornavasso 5071_1_B drilling site (Fig. 5). These differences are on the order of 10 dB and the maximum difference is at frequencies of about 0.1-0.3 Hz, yet part of this difference can be diurnal or seasonal environmental noise variation, and, overall, from an environmental perspective the effects are insignificant.

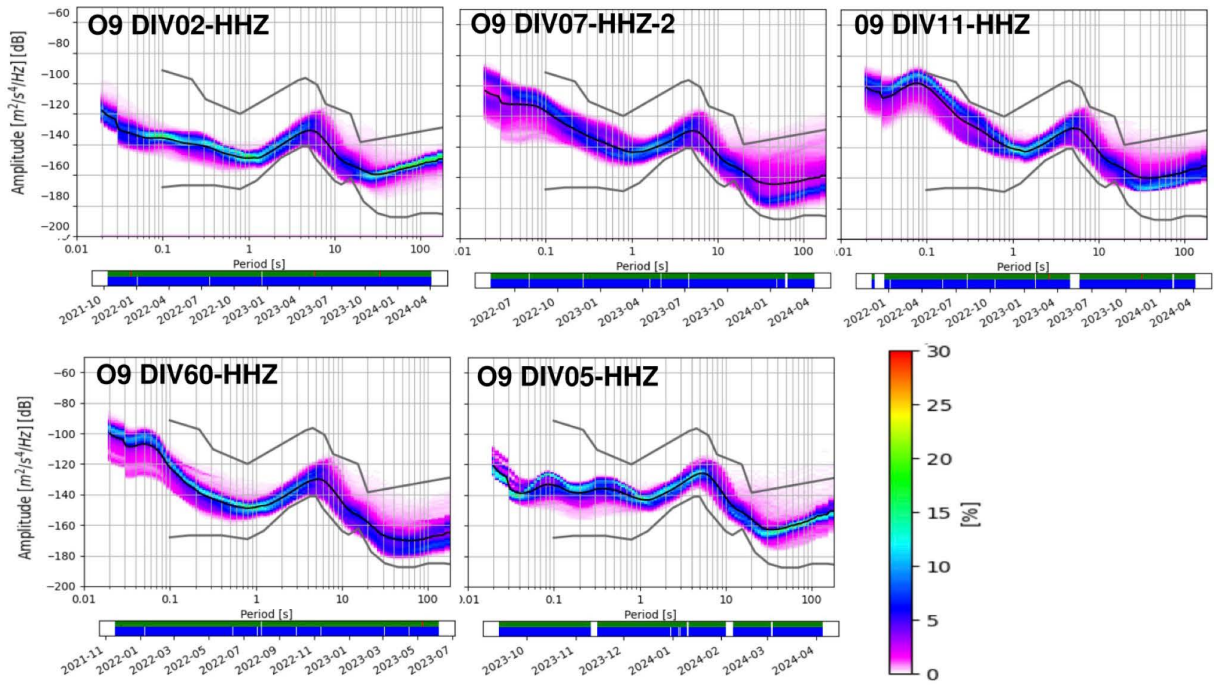

Figure 4. PPSD for the broadband and posthole stations from the 14th of October 2021 until the 17th of June 2024. Top: DIV02 and DIV07 are for a Trillium 120 s, while DIV11 for a Trillium Compact. Bottom: both plots are for the same Trillium 120 Slim Posthole, installed in two different sites, DIV60 and DIV05.

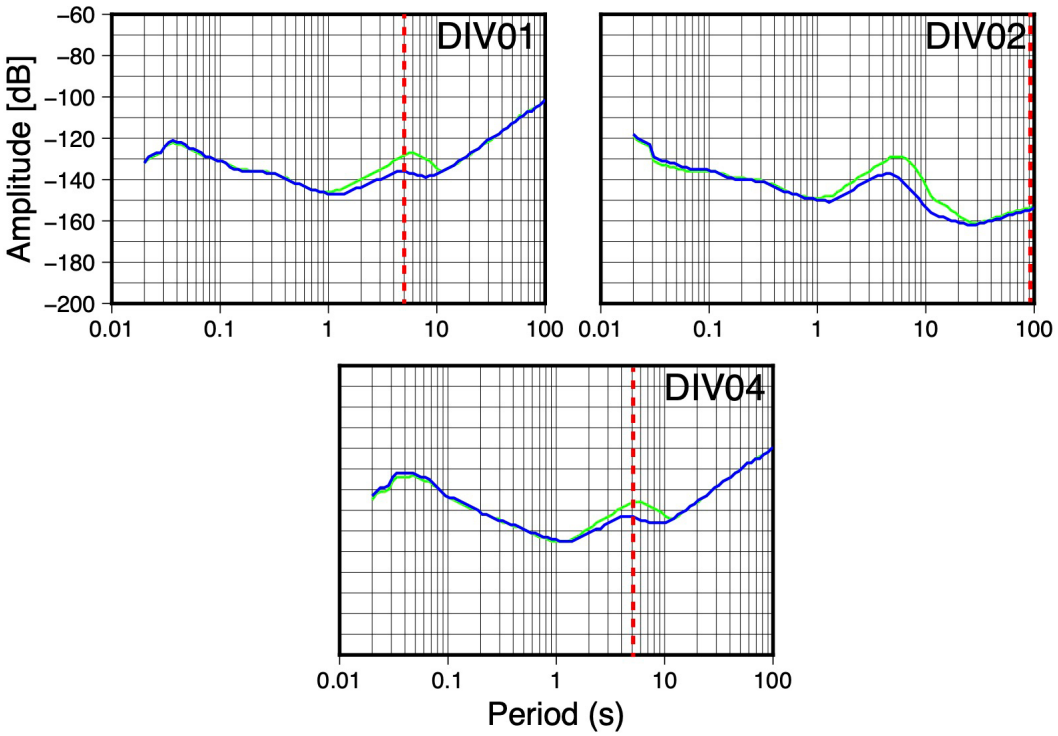

Figure 5. Median of PPSD of the three closest stations to hole 5071_1_B, the first drill site, during the drilling activities (green lines) and as a reference the same time period before the drilling started (blue lines). Vertical dashed red lines indicate the corner period of each sensor (the portions of the diagram to the right of these lines are meaningless).

4. Description of Seismic Catalog

During the time period when the DIVEnet was operational (2021-2024), for the automatic monitoring and network configuration, SeisComP (Helmholtz and gempa, 2008) was utilized. The real-time waveforms are acquired, archived, and processed to identify phase arrivals and associated to locate events. The incoming data are filtered with a 4 poles Butterworth filter between 4 and 20 Hz and then passed by the detection system, using the STA/LTA (short-time-average through long-time-average trigger) values for local networks devoted to microseismicity related to anthropic activities, i.e 0.1 and 5 s. All the earthquakes automatically located are then subsequently verified manually (two examples are shown in the supplementary material, Fig. S2).

The gathered catalogue includes 612 events recorded in the broader region (longitude: 6.5°E to 10°E, latitude: 45°N to 47°N) between November 1, 2021, and June 17, 2024. Event depths ranged from 0 to 59 km (mean error 1.9 km), with magnitudes between 0.2 to 4.0 MLv (mean error 0.3) (Fig. 6). The majority of these events occurred at depths of less than 10 km and had magnitudes between 1 and 2 MLv.

Most events occurred along major fault zones in Switzerland (e.g., the Rhône-Simplon Fault system in the Valais) or in Italy, along the Canavese Line and the Cossato-Mergozzo-Brissago Line (Fig. 1). Beneath the Alps, most earthquakes are shallow, occurring at depths between 3 and 10-15 km (Fig. 7). In contrast, events in the Po Plain reach depths of down to 40 km (Fig. 7). A comparison with the AlpArray earthquake catalogue (Bagagli et al., 2022) reveals similar earthquake locations, despite the AlpArray Seismic Network (Hetényi et al., 2018) covering a greater region and a different recording period (2016-2019). However, the AlpArray dataset recovered less microseismicity, even though it included events with magnitudes as low as 0.4 MLv . This difference may be attributed to their use of an automated procedure for event detection, without subsequent manual review, and the sparser station spacing compared to DIVEnet.

The Swiss Seismological Service (SED) recorded 2,861 earthquakes during the same timeframe as DIVEnet's operation (Fig. 7) in the same region. Despite the SED catalogue extending only as far south as 45.5°N latitude, it was particularly effective in detecting events near the Rhône-Simplon Fault system and the Penninic Front, locating more earthquakes in these areas compared to the DIVEnet network, since they were outside of the monitoring

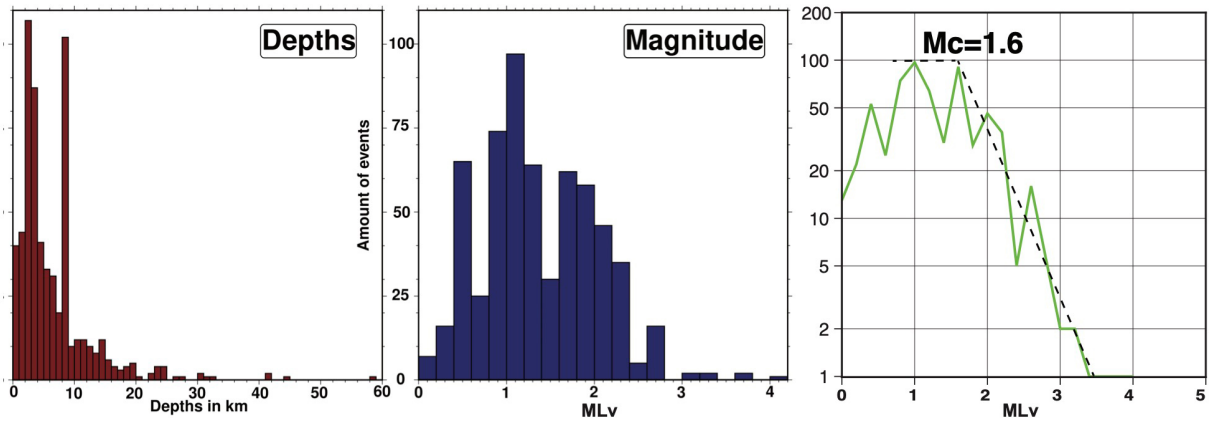

Figure 6. Histograms of hypocentral depths distribution (left) and magnitude (center), and cumulative plot of magnitudes (right), with Mc, for the entire DIVEnet catalog.

network of this study. It is worth noting that SED has been using station DIV07 data since its installation to enhance their network coverage. The Italian Seismological Service (INGV) reported 541 events in the same timeframe and region, but appeared to locate earthquakes approximately 5 to 10 km deeper than those identified by SED or this study, certainly due to the different velocity models used for localization (Fig. 7). Furthermore, the national INGV network struggled to locate some earthquakes in central areas of the northern Po Plain and in Swiss border regions near Maggiore and Orta lakes, and this is possibly due to a different amount of available stations and the

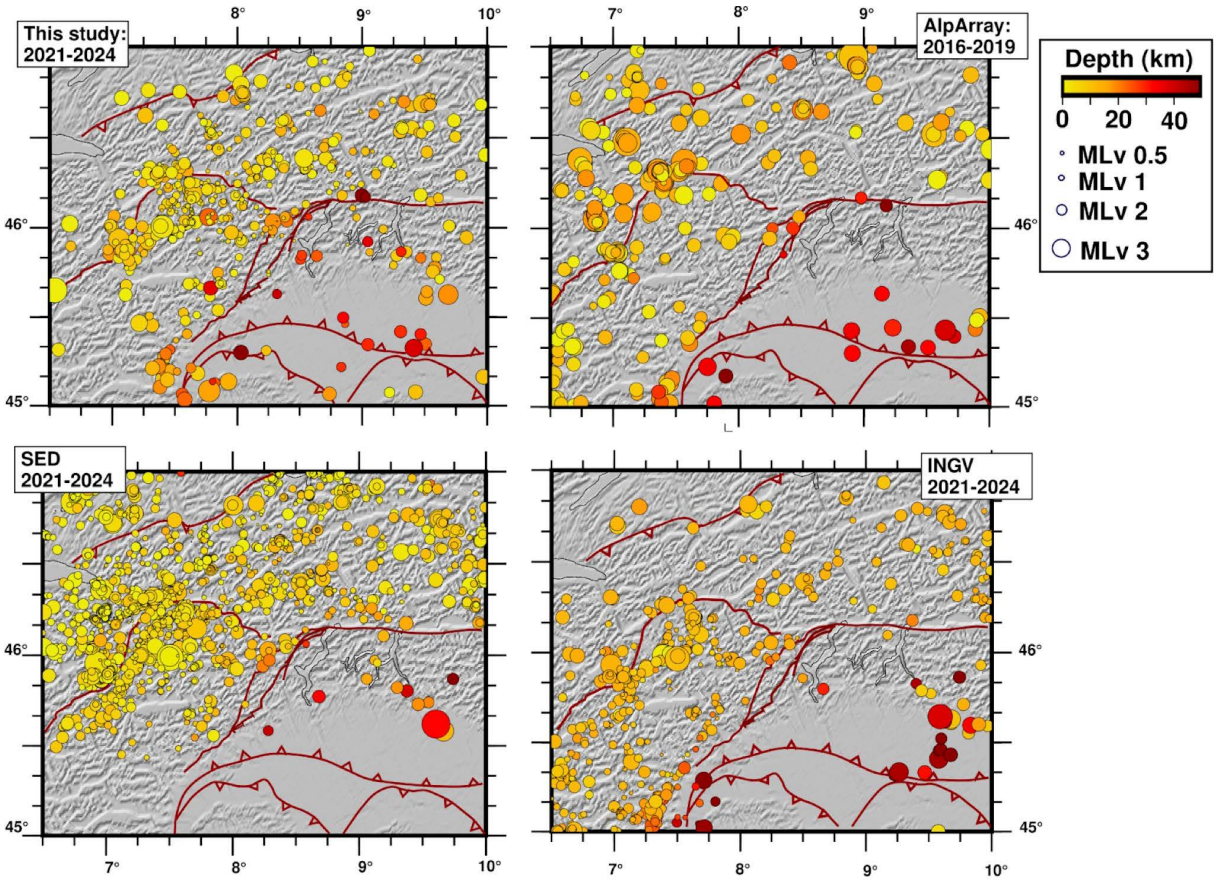

Figure 7. Event locations with their corresponding depths (color) and magnitude (size of circle) of this study, the AlpArray catalogue (Bagagli et al., 2022), the SED catalogue (http://seismo.ethz.ch/en/home, cutoff at 45.5°N), and the INGV catalogue (https://terremoti.ingv.it). Faults are as in Fig. 1.

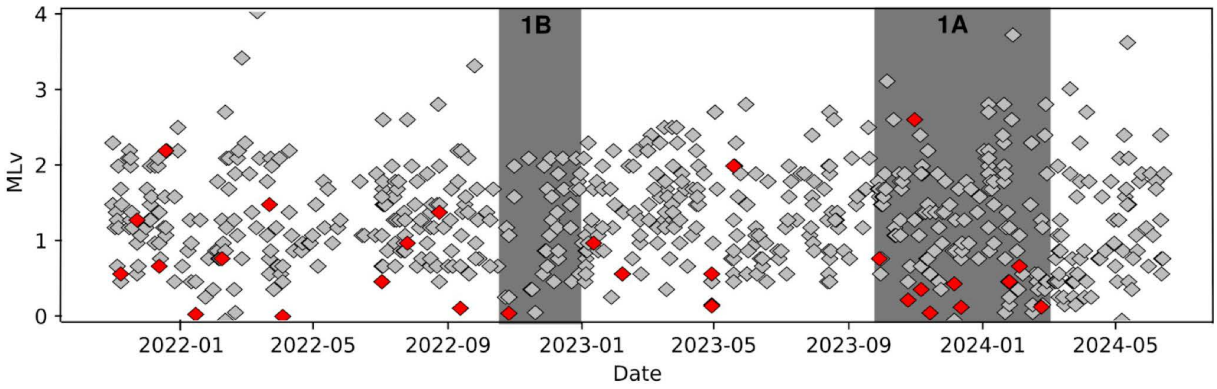

Figure 8. Recorded and located events in the study region with their respective magnitudes over time. Events located in the region closer to drill sites (Fig. 9) are in red, in grey in the background the entire seismicity located in the broader study region (Fig. 7). The dark grey bands represent the drilling times.

possible low quality of data in the Po Plain. In general DIVEnet has clearly improved the detection of the small, local seismicity with respect to the INGV and SED networks, at least in the area within the network (Fig. 9).

Figure 8 shows the time evolution of the catalogue established in this study. It shows that in general seismicity remains stable and continuous, with no significant increase during the drilling phases with respect to earthquakes detected and located before, between and after the drilling activities.

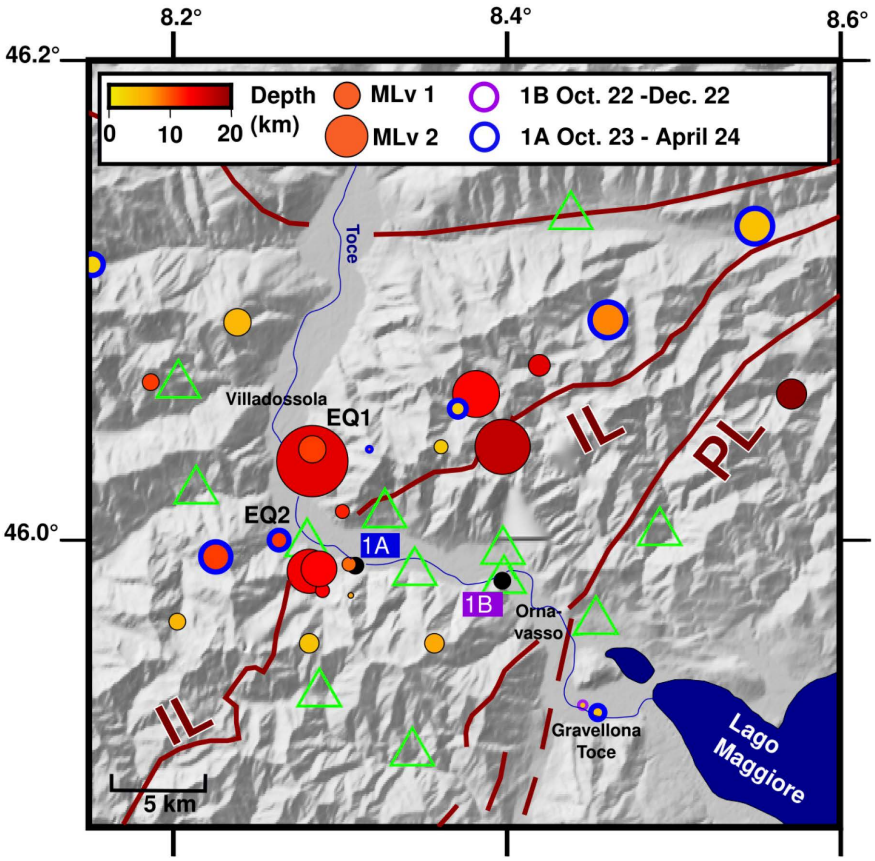

Figure 9. All events (28) occurring inside DIVEnet from October 2021 until the end of the DIVEnet activity. Purple and blue circle contours mean that the respective events occurred during a respective borehole's drilling activities. The Insubric Line is marked with a bolder font and IL. Two example events are shown in the supplementary material (Fig. S2) and labeled on the map as EQ1 and EQ2. Borehole 5071_1_B was drilled Oct.-Dec. 2022, while 5071_1_A started to be drilled in Oct. 2023 and finished on 09.04.2024 at 909 m depth.

In close proximity to the boreholes (longitude: 8.15°E to 8.60°E, latitude: 45.88°N to 46.20°N) only 28 events were recorded (Fig. 9). This result is in agreement with the low seismicity rate of this area. Event depths ranged from 3.5 to 23 km (mean error 0.75 km), with magnitudes ranging from 0.0 to 2.6 MLv (mean error 0.3). Earthquakes larger than 1 MLv along the Insubric line tend to occur at depths between 10 and 20 km. Two small events just west of Maggiore Lake, near Gravellona Toce, coincide with the location of a quarry, suggesting they are quarry blasts. One of these events, with a magnitude of 0.3 MLv, occurred during the first 2-month drilling phase.

The second borehole's drilling phase was longer (5 months), coinciding with a more intense (for the region) activity along the Insubric line. However, the events are evenly distributed in space and time, and are clearly similar to those that occurred before, between, and after the drilling activities. Thus, we interpret these events as tectonic natural earthquakes along the subvertical Insubric line, which dips towards the North-West (Fig. 9).

As already noted for the larger region (Fig. 7), earthquakes are located somewhat differently, particularly in terms of their location and depth, depending on the examined catalog. Figure 10 highlights these differences. While the DIVEnet network recorded 28 events, the SED recorded 14, and INGV recorded 8 events during the same time period. In particular, events smaller than 0.6 MLv (nine events in this study) seem to be missing from both permanent monitoring services. The inclusion of DIV07 in their monitoring system helped the SED recover most of the larger events, with similar locations and depths as reported in this study, but was not enough to also include microearthquakes.

Throughout the drilling period, continuous monitoring of radon (^{222}Rn) revealed short-term spikes ranging from background levels of approximately 50 Bq/m^3 to peaks of up to 1500 Bq/m^3 (Dutoit et al., 2025). Such spikes were common throughout the drilling phase of the first borehole, whereas elevated radon levels during the second drilling phase were only observed at depths of 250-300 m and below 650 m. These increases were closely correlated with active drilling operations and consistently returned to background levels during inactive periods (e.g. overnight or at midday), indicating an operational rather than tectonic origin (Dutoit et al., 2025). Radon concentrations comparable to those observed here are considered moderate in comparison to some tectonically

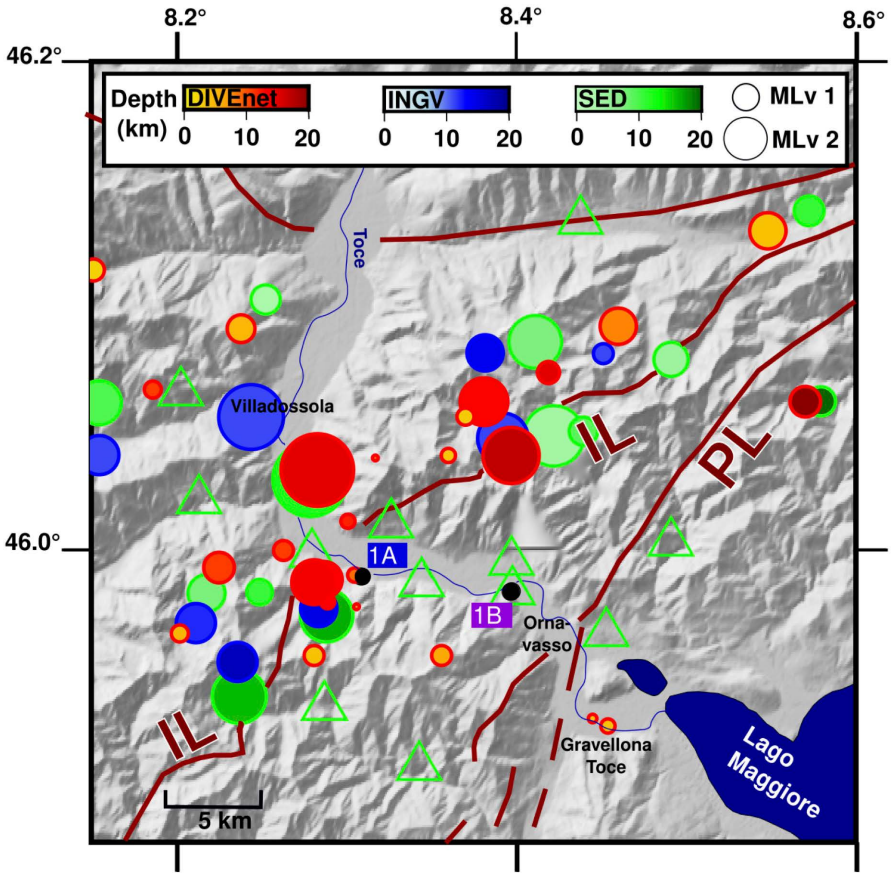

Figure 10. Located earthquakes in close proximity to DIVEnet (yellow to red colors scale for depth) and the comparison to the INGV (blue color scale) and SED earthquake catalogs (green color scale).

active regions (e.g. Xuan et al., 2020; Benà et al., 2022). During intervals of elevated radon, no abnormal seismicity was recorded with only a few microearthquakes with magnitudes below 1.0, consistent with regional background levels. Furthermore, no anomalous radon-helium correlations or fluid inflows indicative of deep, fault-related degassing were observed in logs or occluded gas analyses. These findings support the conclusion that the radon variations were driven solely by drilling disturbances and were not associated with any tectonic activity.

5. Recovering the orientation of the borehole sensor at DIV05

As mentioned above, once the first borehole (5071_1_B) was completed and the site restored, a broadband borehole seismometer was installed at 252 m depth below surface in the near vertical hole. This station operated up to the summer of 2024 for nearly one year. The seismometer was fixed with its own clamping system, and the steel cable and the data cable (that have been tightened together every 15 m) have been slightly released to avoid vibrations between the surface and the sensor. The data recording system, powered by a solar panel, has been installed at the surface. As the borehole was filled with water naturally, a sealing system was prepared at the well head which let the cables pass through, minimising the water exit. Further details of the installation and recovery are described in the DIVE Operational Report (in preparation). From an observational seismology point of view, the main exercise was to determine the orientation of the horizontal components, while the vertical has shown immediately to be essentially vertical, also when compared with data from the rest of the DIVEnet stations.

To ensure a constrained result of the horizontal components' orientation, another three-component seismometer has been installed for a short time at the top of the hole, to be used as a reference with a proper North orientation (named DIV05s). A cross correlation comparison of data recorded by DIV05 and the station at the surface DIV05s gave the first information on the direction of the H1 and H2 horizontal components of the sensor at depth. Several cross correlation comparisons produced the results plotted in the polar histogram of Fig. 11, where the maximum frequency is at 87°. This means that a clockwise rotation of the N component of the surface station by 87° produces a nearly perfect overlap with the DIV05 borehole data, as shown in the example on Fig. 12.

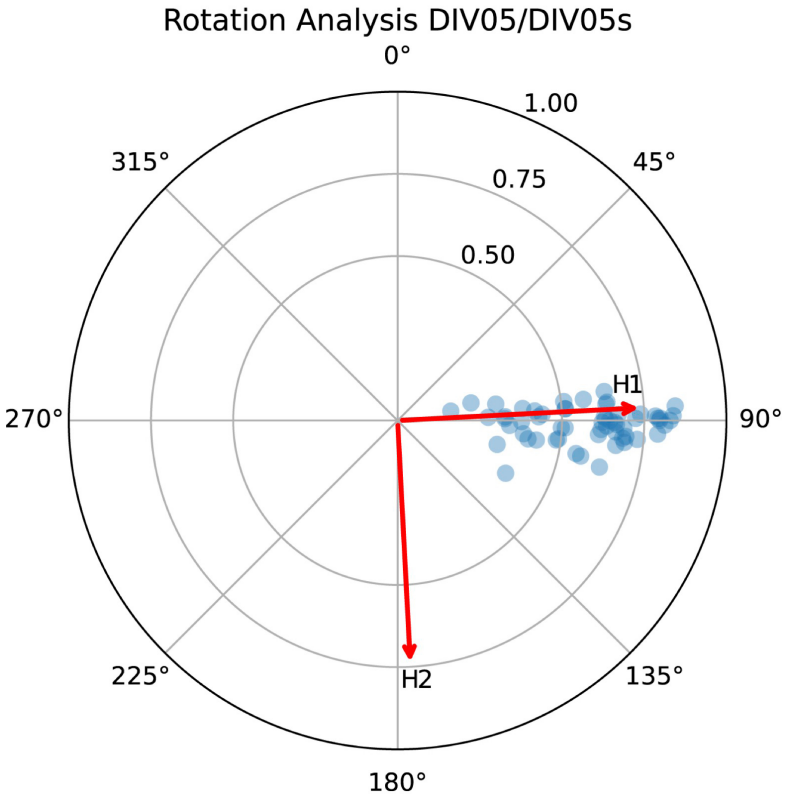

Figure 11. Polar histogram of noise cross-comparisons that has its maximum frequency on the value of 87°, where HH1 points.

To reinforce this result, a similar comparison, but on teleseismic data has been done between waveform recordings from DIV05 and DIV07, another broadband station located at less than 10 km southwest of the borehole (Fig. 2). The result is again clearly good, with a rotation of 87° (Fig. 13).

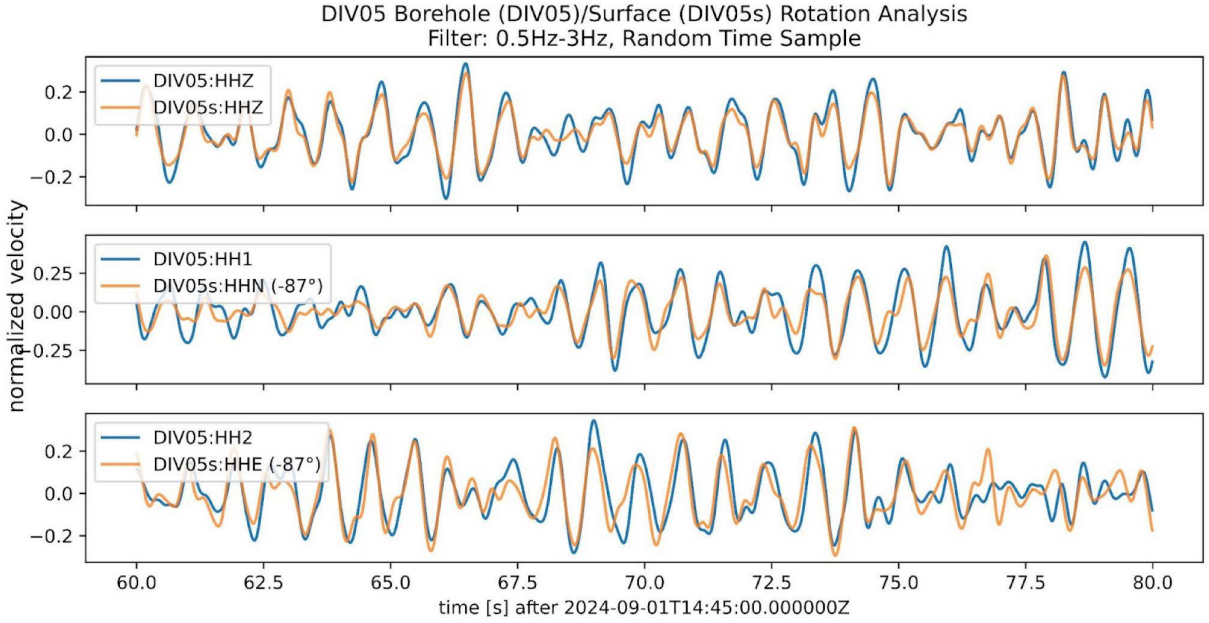

Figure 12. Cross matching of the noise waveforms from DIV05 (sensor in the borehole) and DIV05s (sensor at the surface), after the rotation of −87°. Filter is 0.5 to 3 Hz.

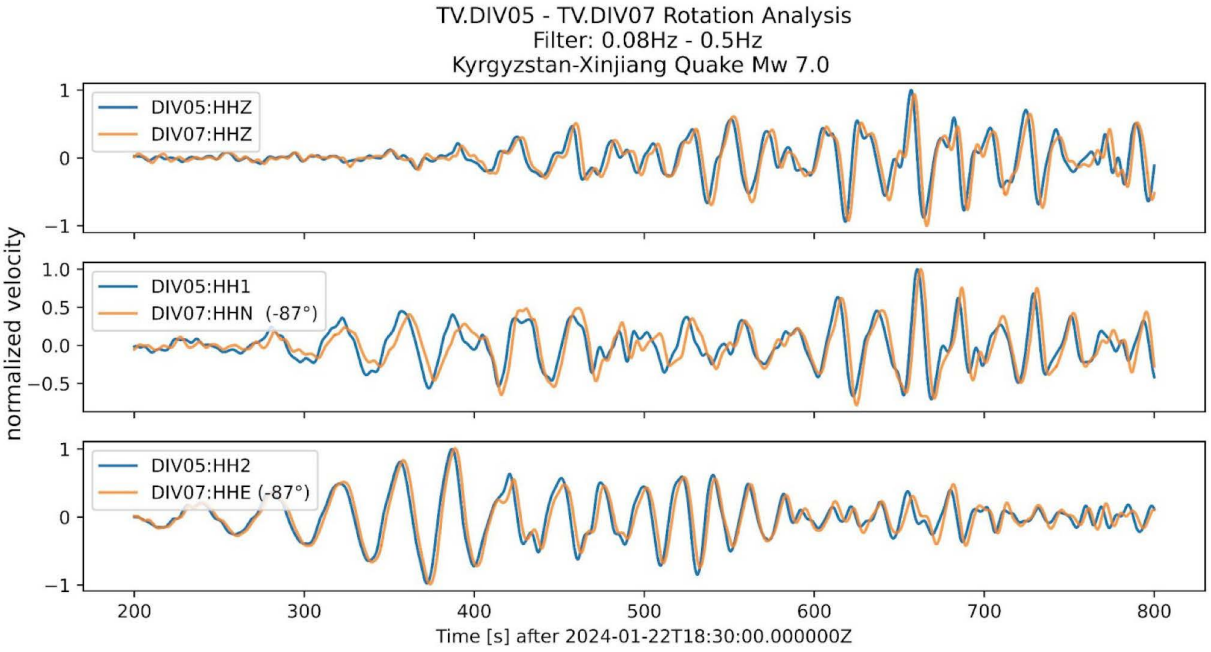

Figure 13. Cross matching of recordings of a teleseismic event after a rotation of −87° of DIV05 data.

To prove the proper recovery of the horizontal components' direction, we also used the AutoStatsQ software (Petersen et al., 2019). AutoStatsQ is a software that uses the Rayleigh waves polarization (period between 20 and 100 s) to recover horizontal component's direction . The result obtained for DIV05 data is −82°, that means an anticlockwise rotation of H1 to overlap the N, e.g. H1 again results striking nearly to the East. Even though the

available good quality events for the test were not so numerous, namely 11 events, the result matches very well the orientation results obtained above.

In conclusion, we consider that the borehole sensor's H1 component points towards 85° ±2° and consequently H2 towards 175° ±2°, nearly south. Metadata will be updated accordingly.

6. Conclusions

The temporary DIVEnet network, designed for the monitoring of scientific drilling activities of the ICDP-DIVE project, worked seamlessly for nearly 3 years. From the use of these stations and some permanent stations a catalog of 611 events with magnitudes ranging from 0.2 to 4.0 MLv has been collected. In the closer area around the drilling sites 28 events with magnitudes ranging from 0.0 to 2.6 MLv have been localised. From the comparison of seismicity recorded before, during, and after the drillings, we do not observe any significant change we can ascribe to anthropic activities. Comparing the seismic activity recorded by DIVEnet with catalogs by SED and INGV during the same time period we observe that the presence of this local temporary network improves the event detection, that means that even only one additional permanent station in this area may be useful.

The installations have been quick and stations located in favorable logistic conditions with a small disadvantage with respect to noise, and the quality of data resulted in a very good level. The unknown direction of the horizontal components of the borehole sensor, installed in the first drilling site after the end of drilling operations, has been recovered with the use of different approaches, applied on noise and teleseismic recordings: at station DIV05 the HH1 component pointed towards 85° ±2° and HH2 towards 175° ±2°.

In conclusion, the main findings we obtained with this local temporary network, are that (1) the occurrence of drilling-induced earthquakes can be excluded, (2) the recorded local seismicity is located along the Insubric Line, despite it being tectonically considered inactive.

All the continuous recordings acquired during the DIVEnet will be carefully revised for local seismicity studies, and it will be used also for local structure studies (e.g. receiver function, seismic anisotropy), where it will be compared with drilling log data (Li et al., 2024) and fiber optic data collected during drilling activities.

Data availability statement. All DIVEnet data (10.7914/ffna-qf89), after 1 year from the dismantling of the temporary network, will be available on EIDA (https://eida.ingv.it) following the FDSN code 9O. In the meanwhile data may be available on demand writing to the corresponding author.

Acknowledgements. The Authors thank local administrations and churches that hosted DIVEnet instruments: Comune di Anzola D'Ossola (DIV01), Comune di Premosello-Chiovenda (DIV02), Comune di Mergozzo (DIV03, DIV04), Parco della ValGrande (DIV12), Comune di Druogno (DIV11), Comune di Valstrona (DIV06, DIV60, DIV07), Comune di Seppiana (DIV08), Comune di Calasca-Castiglione (DIV09), Parrocchia di Pieve Vergonte (DIV01, DIV10).

The Authors thank the Site effect – ESITO laboratory of the Istituto Nazionale di Geofisica e Vulcanologia (https://www.ingv.it/en/monitoraggio-e-infrastrutture/laboratori/laboratorio-effetti-di-sito) for preparing, configuring and providing instrumentation, and generating the output files and state-of-health files. The ESITO Laboratory is part of the Integrated Laboratories for Geosciences and Environment-ILGE of MEET Project (Monitoring Earth's Evolution and Tectonics, https://meet.ingv.it; National Recovery and Resilience Plan (PNRR), Mission 4, Component 2, Investment line 3.1 – project code IR0000025)".

Our thanks go to Carlo Giunchi and other colleagues of INGV-Pisa for their support in the data acquisition process. For the help in the fieldwork we thank Konstantinos Michailos (UNIL). Part of the field and operational costs have been covered by the Swiss National Science Foundation, Grant PP00P2_187199 (project OROG3NY).

To produce the work described, the following software programmes have been used: SeisComP, AutoStatsQ, SAC, GMT (Generic Mapping Tools; Wessel and Smith, 1998).

This study was performed in the framework of the Project INGV Pianeta Dinamico 2023-2025 UNLOCK (code CUP D53J19000170001) funded by the Italian Ministry of University and Research "Fondo finalizzato al rilancio degli investimenti delle amministrazioni centrali dello Stato e allo sviluppo del Paese, legge 145/2018" and of the Project DIVE@INGV, which payed the post doc position of J.M. Confal.

References

Bagagli, M., I. Molinari, T. Diehl, E. Kissling and D. Giardini (2022). The AlpArray research seismicity-catalogue. Geophys. J. Int., 231, 2, 921-943, doi:10.1093/gji/ggac226.

Benà, E., G. Ciotoli, L. Ruggiero, C. Coletti et al. (2022). Evaluation of tectonically enhanced radon in fault zones by quantification of the radon activity index, Sci. Rep., 12, 1, 21586.

Berger, A., I. Mercolli, N. Kapferer and B. Fügenschuh (2012). Single and double exhumation of fault blocks in the internal Sesia-Lanzo Zone and the Ivrea-Verbano Zone (Biella, Italy), Int. J. Earth Sci., 101, 1877-1894.

Béthoux, N., C. Sue, A. Paul, J. Virieux et al. (2007). Local tomography and focal mechanisms in the south-western Alps: Comparison of methods and tectonic implications, Tectonophys., 432, 1-19.

Boriani, A., L. Burlini and R. Sacchi (1990). The Cossato Mergozzo Brissago Line and the Pogallo Line (southern Alps, N-Italy) and their relationships with the late-hercynian magmatic and metamorphic events, Tectonophys., 182, 91-102.

Brack, P., P. Ulmer and S. M. Schmi (2010). A crustal magmatic system from the Earth mantle to the Permian surface – Field trip to the area of lower Valsesia and Val d'Ossola (Massiccio dei Laghi, Southern Alps, Northern Italy), Swiss Bull. Angew. Geol., 15, 3-21.

Dutoit, H., L. Truche, F. V. Donzé, T. Wiersberg et al. (2025). Continuous real-time detection of H2, He, and 222Rn while drilling DIVE-1 boreholes (ICDP) indicates deep fracture fluid migration in crystalline rocks. Geochemistry, Geophysics, Geosystems, 26, 5, e2025GC012168.

Garde, A. A., A. Boriani and E. V. Sørensen (2015). Crustal modelling of the Ivrea-Verbano zone in northern Italy re-examined: coseismic cataclasis versus extensional shear zones and sideways rotation., Tectonophys., 662, 291-311.

Greenwood, A., G. Hetényi, L. Baron, A. Zanetti et al. (2024). Active seismic surveys for drilling target characterisation in Ossola Valley: International Continental Scientific Drilling Program (ICDP) project Drilling the Ivrea-Verbano zonE (DIVE) phase, I. Sci Drill, 33, 219-236. doi:10.5194/sd-33-219-2024.

Handy, M. R. (1987). The structure, age and kinematics of the Pogallo fault zone, southern Alps, northwestern Italy, Eclog. Geol. Helvet., 80, 593-632.

Helmholtz Centre Potsdam GFZ German Research Centre for Geosciences and gempa GmbH (2008). The SeisComP seismological software package. GFZ Data Services. doi:10.5880/GFZ.2.4.2020.003.

Hetényi, G., I. Molinari, J. Clinton et al. (2018). The AlpArray Seismic Network: a large-scale European experiment to image the Alpine orogeny. Surveys in Geophysics, 39, 1009-1033. doi:10.1007/s10712-018-9472-4.

Kissling, E. (1984). Three dimensional gravity model of the northern Ivrea-Verbano zone. In: J. J. Wagner and S. Mueller (eds) Geomagnetic and gravimetric studies of the Ivrea zone, 53-61, Swiss Comm. Geophysics. Attinger SA, Neuchâtel.

Li, J., E. Caspari, A. Greenwood, S. Pierdominici, K. Lemke et al. (2024). Integrated rock mass characterization of the lower continental crust along the ICDP-DIVE 5071_1_B borehole in the Ivrea-Verbano Zone, Geochem. Geophys. Geosyst., doi:10.1029/2024GC011707.

Masson, F., J. Verdun, R. Bayer and N. Debeglia (1999). Une nouvelle carte gravimétrique des Alpes occidentales et ses conséquences structurales et tectoniques, Comptes Rendus de l'Académie des Sciences – Series IIA – Earth Planet. Sci., 329, 865-871.

Nicolas, A., A. Hirn, R. Nicolich, R. Polino and E.-C. W. Group (1990). Lithospheric wedging in the Western Alps inferred from the ECORS-CROP traverse, Geol., 18, 587-590.

Paul, A., M. Cattaneo, F. Thouvenot, D. Spallarossa et al. (2001). A three-dimensional crustal velocity model of the south-western Alps from local earthquake tomography, Journal of Geophysical Research, 106, 19367-19389.

Petersen, G. M., S. Cesca, M. Kriegerowski (2019). Automated Quality Control for Large Seismic Networks: Implementation and Application to the AlpArray Seismic Network, Seismol. Res. Lett., 90, 3, 1177-1190, doi:10.1785/0220180342.

Petri, B., T. Duretz, G. Mohn, S. M. Schmalholz et al. (2019). Thinning mechanisms of heterogeneous continental lithosphere, Earth Planet. Sci. Lett., 512, 147-162.

Pistone, M., L. Ziberna, G. Hetényi, M. Scarponi et al. (2020). Joint geophysical-petrological modeling on the Ivrea geophysical body beneath Valsesia, Italy: Constraints on the continental lower crust, Geochem., Geophys., Geosys., 21, e2020GC009397, doi:10.1029/2020GC009397.

Quick, J. E., S. Sinigoi, L. Negrini, G. Demarchi and A. Mayer (1992). Syn-magmatic deformation in the underplated igneous complex of the Ivrea-Verbano Zone, Geol., 20, 613-616.

Rovida, A., A. Antonucci and M. Locati (2022). The European Preinstrumental Earthquake Catalogue EPICA, the 1000-1899 catalogue for the European Seismic Hazard Model 2020, Earth Sys. Sci. Data, 14, 5213-5231, doi:10.5194/essd-14-5213-2022.

Redler, C., T. E. Johnson, R. W. White and B. Kunz (2012). Phase equilibrium constraints on a deep crustal metamorphic field gradient: Metapelitic rocks from the Ivrea Zone (NW Italy). J. Metamorphic Geol., 30, 235-254.

Salisbury, M. H. and D. M. Fountain (Eds.) (1990). Exposed cross-sections of the continental crust (NATO ASI Series C, Vol. 317). Dordrecht, The Netherlands and Boston, MA and London, UK: Kluwer.

Scarponi, M., G. Hetényi, T. Berthet, L. Baron et al. (2020). New gravity data and 3-D density model constraints on the Ivrea Geophysical Body (Western Alps), Geophys. J. Int., 222, 3, 1977-1991.

Scarponi, M., G. Hetényi, J. Plomerová, S. Solarino et al. (2021). Joint seismic and gravity data inversion to image intra-crustal structures: the Ivrea Geophysical Body along the Val Sesia profile (Piedmont, Italy), Front. Earth Sci., 9, doi:10.3389/feart.2021.671412.

Scarponi, M., J. Kvapil, J. Plomerová, S. Solarino and G. Hetényi (2024). New constraints on the shear wave velocity structure of the Ivrea geophysical body from seismic ambient noise tomography (Ivrea-Verbano Zone, Alps), Geophys. J. Int., 236, 1089-1105, doi:10.1093/gji/ggad470.

Schmid, S. M., A. Zingg and M. Handy (1987). The kinematics of movements along the Insubric Line and the emplacement of the Ivrea Zone, Tectonophysics, 135, 47-66.

Schmid, S. M., B. Fügenschuh, E. Kissling and R. Schuster (2004). Tectonic map and overall architecture of the Alpine orogen, Eclogae Geologicae Helvetiae, 97, 93-117.

Schmid, S. M., E. Kissling, T. Diehl, D. J. van Hinsbergen and G. Molli (2017). Ivrea mantle wedge, arc of the Western Alps, and kinematic evolution of the Alps-Apennines orogenic system, Swiss J. Geosci., 110, 581-612.

Snoke, A. W., T. J. Kalakay, J. E. Quick and S. Sinigoi (1999). Development of a deep-crustal shear zone in response to syntectonic intrusion of mafic magma into the lower crust, Ivrea-Verbano Zone, Italy, Earth Planet. Sci. Lett., 166, 31-45.

Spicher, A. (Ed.). (1968). Symposium "Zone Ivrea-Verbano". Schweizerische Mineralogische und Petrographische Mitteilungen, 48, 1-355.

Wessel, P. and W. H. Smith (1998). New, improved version of Generic Mapping Tools released. EOS Trans. Am. Geophys. Union 79, 47, 579. doi:10.1029/98EO00426, 579.

Xuan, P. T., N. A. Duong, V. Van Chinh, P. T. Dang et al. (2020). Soil gas radon measurement for identifying active faults in Thua Thien hue (Vietnam). J. Geosci. Environ. Protec., 8, 7, 44.

***CORRESPONDING AUTHOR: Silvia PONDRELLI**,
INGV, Sezione di Bologna
e-mail: silvia.pondrelli@ingv.it